

Supporting Information
for

4,4'-difluorobenzhydryl-modified bis(imino)pyridyliron(II) chlorides as thermally stable precatalysts for strictly linear polyethylenes with narrow dispersity

Qiuyue Zhang,^{a,b} Randi Zhang,^{a,b} Mingyang Han,^{a,b} Wenhong Yang,^{*a} Tongling Liang^a and Wen-Hua Sun^{a,b,c*}

^a Key Laboratory of Engineering Plastics and Beijing National Laboratory for Molecular Sciences, Institute of Chemistry, Chinese Academy of Sciences, Beijing 100190, China. E-mail: whyang@iccas.ac.cn or whsun@iccas.ac.cn; Fax: +86-10-62618239; Tel: +86-10-62557955.

^b CAS Research/Education Center for Excellence in Molecular Sciences and International School, University of Chinese Academy of Sciences, Beijing 100049, China.

^c State Key Laboratory for Oxo Synthesis and Selective Oxidation, Lanzhou Institute of Chemical Physics, Chinese Academy of Sciences, Lanzhou 730000, China.

Contents

- 1. Figure S1.** ¹H NMR spectrum of **Fe2** (recorded in CDCl₃ at ambient temperature).
- 2. Figure S2.** ¹H NMR spectrum of **Fe3** (recorded in CDCl₃ at ambient temperature).
- 3. Figure S3.** ¹H NMR spectrum of **Fe4** (recorded in CDCl₃ at ambient temperature).
- 4. Figure S4.** ¹H NMR spectrum of **Fe5** (recorded in CDCl₃ at ambient temperature).
- 5. Figure S5.** ¹H NMR spectrum of **Fe6** (recorded in CDCl₃ at ambient temperature).
- 6. Figure S6.** ¹⁹F NMR spectra of **Fe1** – **Fe6** (recorded in CDCl₃ at ambient temperature).
- 7. Figure S7.** GPC curves (a) and activity and *M_w* of the resultant polyethylene produced using **Fe1**/MMAO vs. various Al/Fe ratios (entries 5, 8–12, Table 3).
- 8. Figure S8.** GPC curves (a) and mass of polymer and *M_w* of the resultant polyethylene produced using **Fe1**/MMAO vs. different running time (entries 11, 13–16, Table 3).
- 9. Figure S9.** Catalytic activity of **Fe1**/MAO and **Fe1**/MMAO catalytic systems vs. different running time (entries 9, 12–15, Table 2 and entries 11, 13–16, Table 3).
- 10. Figure S10.** Definition of open cone angle (θ) of complex. (Computational Part)
- 11. Table S1.** Crystal data and structure refinement for **Fe1** and **Fe6**.
- 12. Table S2.** The calculated values of effective net charge (Q_{eff}) and open cone angle (θ) for four complexes, respectively. (Computational Part)

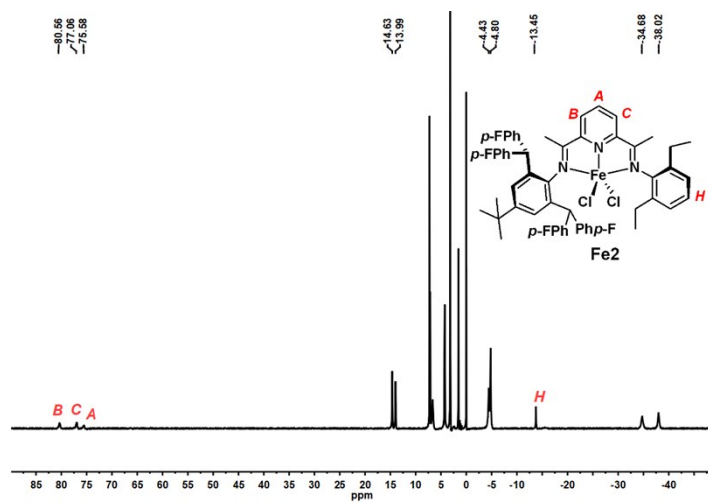


Figure S1. ^1H NMR spectrum of **Fe2** (recorded in CDCl_3 at ambient temperature).

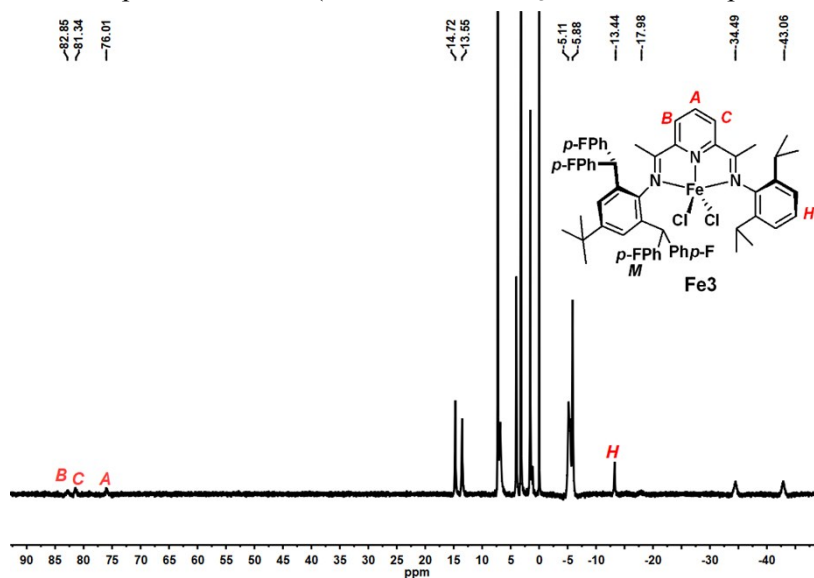


Figure S2. ^1H NMR spectrum of **Fe3** (recorded in CDCl_3 at ambient temperature).

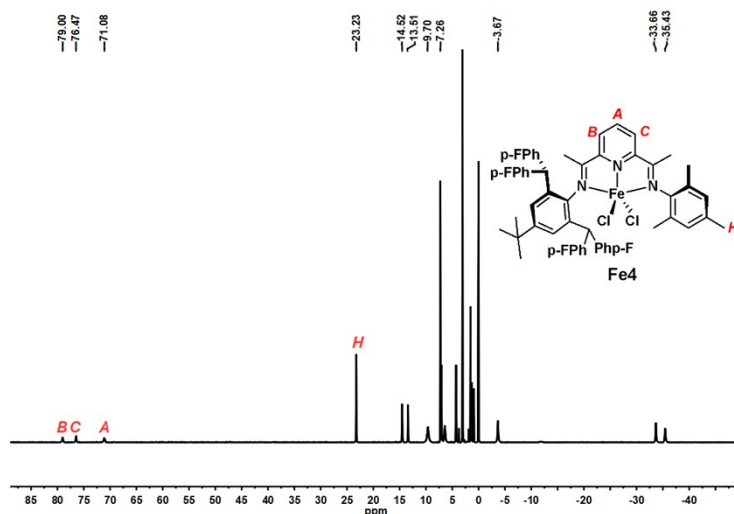


Figure S3. ^1H NMR spectrum of **Fe4** (recorded in CDCl_3 at ambient temperature).

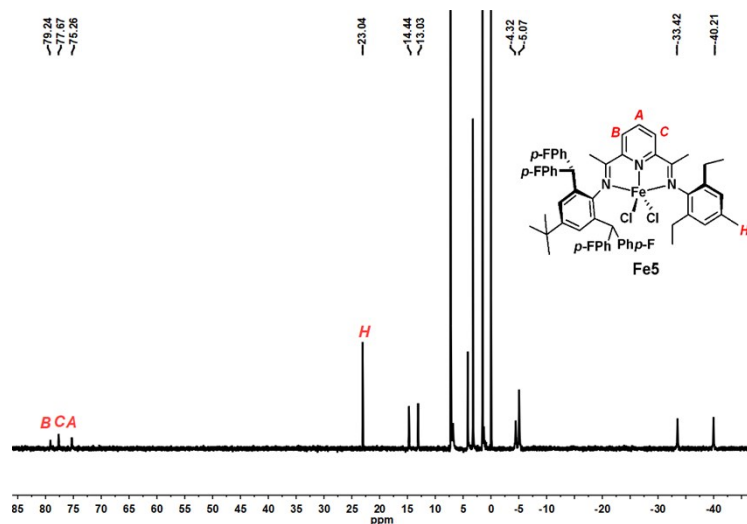


Figure S4. ^1H NMR spectrum of **Fe5** (recorded in CDCl_3 at ambient temperature).

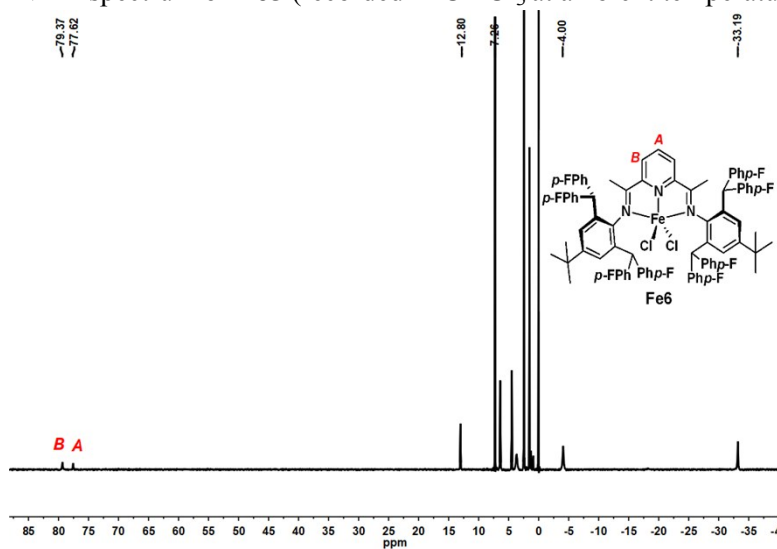


Figure S5. ^1H NMR spectrum of **Fe6** (recorded in CDCl_3 at ambient temperature).

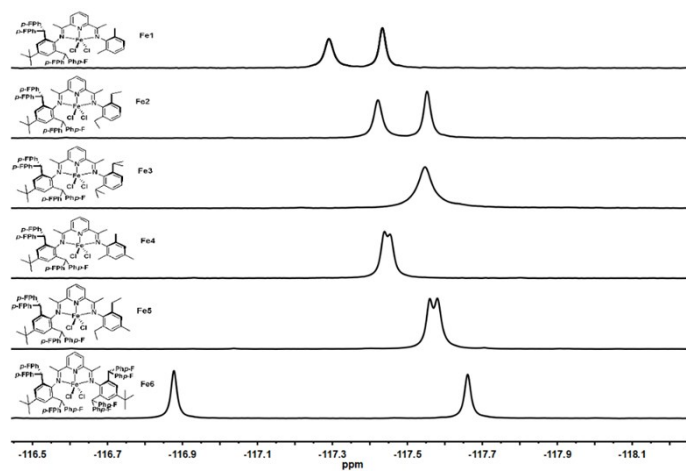


Figure S6. ^{19}F NMR spectra of **Fe1** – **Fe6** (recorded in CDCl_3 at ambient temperature).

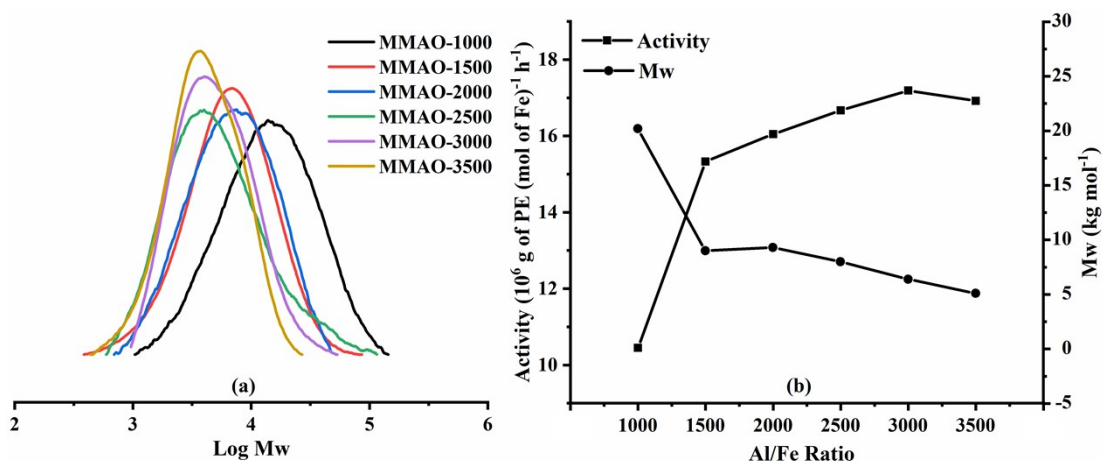


Figure S7. GPC curves (a) and activity and M_w of the resultant polyethylene produced using Fe1/MMAO vs. various Al/Fe ratios (b) (entries 5, 8–12, Table 3).

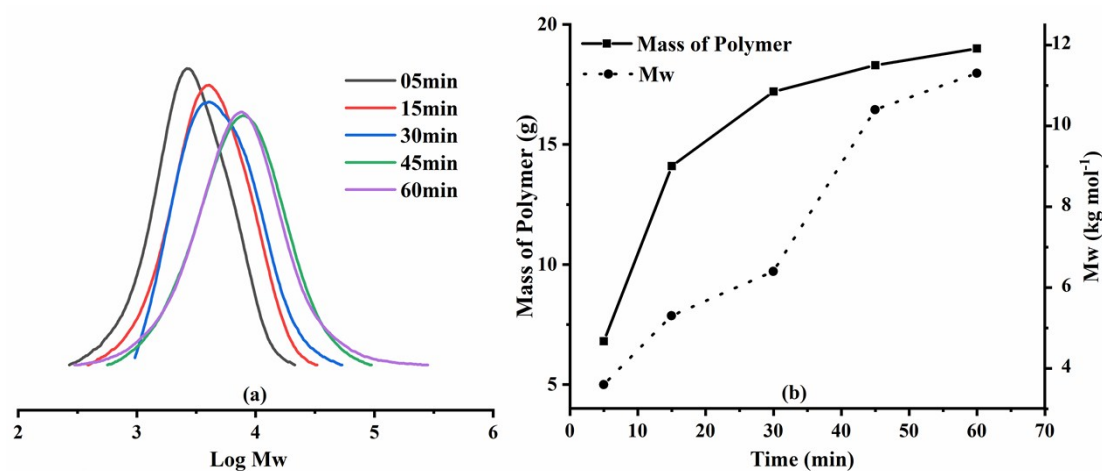


Figure S8. GPC curves (a) and mass of polymer and M_w of the resultant polyethylene produced using Fe1/MMAO vs. different running time (b) (entries 11, 13–16, Table 3).

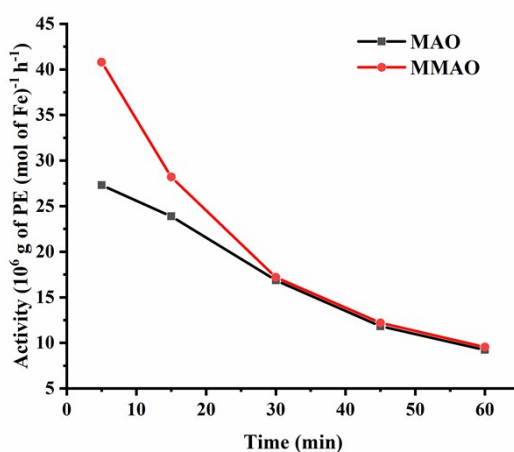


Figure S9. Catalytic activity of Fe1/MAO and Fe1/MMAO catalytic systems vs. different running time (entries 9, 12–15, Table 2 and entries 11, 13–16, Table 3).

Table S1. Crystal data and structure refinement for **Fe1** and **Fe6**.

Identification code	Fe1	Fe6
CCDC number	1976469	1976470
Empirical formula	C ₅₃ H ₄₇ Cl ₂ F ₄ FeN ₃	C ₈₁ H ₆₇ Cl ₂ F ₈ FeN ₃
Formula weight	928.68	1361.12
Temperature/K	173.1500	173.1500
Crystal system	triclinic	monoclinic
Space group	P-1	P2 ₁ /c
a/Å	10.0392(2)	15.8334(10)
b/Å	11.7966(2)	16.7550(7)
c/Å	21.7852(3)	28.0601(12)
α/°	105.5070(10)	90
β/°	94.7070(10)	100.806(5)
γ/°	105.747(2)	90
Volume/Å ³	2359.28(7)	7312.0(6)
Z	2	4
ρ _{calc} /cm ³	1.307	1.236
μ/mm ⁻¹	0.487	0.344
F(000)	964.0	2824.0
Crystal size/mm ³	0.283 × 0.099 × 0.072	0.324 × 0.083 × 0.033
Radiation	MoKα (λ = 0.71073)	MoKα (λ = 0.71073)
2θ range for data collection/°	3.682 to 62.998	3.574 to 63.048
Index ranges	-14 ≤ h ≤ 14, -17 ≤ k ≤ 17, -31 ≤ l ≤ 31	-21 ≤ h ≤ 23, -23 ≤ k ≤ 24, -41 ≤ l ≤ 39
Reflections collected	30950	57774
Independent reflections	13946 [R _{int} = 0.0315, R _{sigma} = 0.0466]	22020 [R _{int} = 0.1513, R _{sigma} = 0.2916]
Data/restraints/parameters	13946/0/575	22020/0/864
Goodness-of-fit on F ²	1.043	0.942
Final R indexes [I ≥ 2σ(I)]	R ₁ = 0.0522, wR ₂ = 0.1204	R ₁ = 0.0982, wR ₂ = 0.1744
Final R indexes [all data]	R ₁ = 0.0744, wR ₂ = 0.1340	R ₁ = 0.2665, wR ₂ = 0.2417
Largest diff. peak/hole / e Å ⁻³	0.87/-0.38	0.53/-0.56

Computational Part

To optimize the geometries of the four complexes in Figure 13, molecular mechanics (MM) [1] calculation has been performed based on our previous reports [2]. Dreiding force field is used in Forcite program package [3]. Since there is no atom type of the central metal and the coordinated nitrogen atoms, we add the corresponding information of bond lengths and bond angles into the force fields on the basis of the experimental crystal data. The convergence tolerances of the force and energy are $0.5 \text{ kcal}\cdot\text{mol}^{-1}\cdot\text{\AA}^{-1}$ and $0.001 \text{ kcal}\cdot\text{mol}^{-1}$, respectively. The cutoff distance of cubic spline is 1.25 nm. To describe electrostatic and van der Waals interactions, atom based Summation and Truncation methods are used, respectively. Comparison between the optimized structure and the crystal data for complex $\mathbf{E}_{t\text{-Bu}}$ (**Fe1**) was shown in Table S2, clearly indicating the reasonable optimized result with lower standardized deviation values for both bond lengths and bond angles.

In our previous studies, there are seven descriptors from both electronic and steric effects which can reflect the influence of ligand's structure [4]. Herein, we choose two of them, which play the dominant role in determining the activity and molecular weight properties of complex, including effective net charge (Q_{eff}) and open cone angle (θ). For electronic effect, effective net charge (Q_{eff}) is the difference between the net charge on central metal atom and the difference of net charge on two halogen atoms bonding with the metal in the complex, calculating by equation S1 [5].

$$Q_{\text{eff}} = Q_{\text{CM}} - \Delta Q_{\text{halogens}} \quad \text{S1}$$

where Q_{CM} is the net charge present on central metal atom, and $\Delta Q_{\text{halogens}}$ represents the difference value of the net charges present on halogen atoms attached to central metal atom.

For steric effect, open cone angle (θ) is calculated in the same manner as previous study [6] by using equation S2.

$$\theta = 360^\circ - \left[\angle C_1 + \arcsin \frac{r_2}{L_2} + \angle D_1 + \arcsin \frac{r_1}{L_1} \right] \quad \text{S2}$$

where $\angle C_1$, $\angle D_1$ and L_1 , L_2 are obtained from the optimized geometry structure of

precatalyst, r_1 and r_2 are the van der Waals radius of the outmost atom as shown in Figure S10.

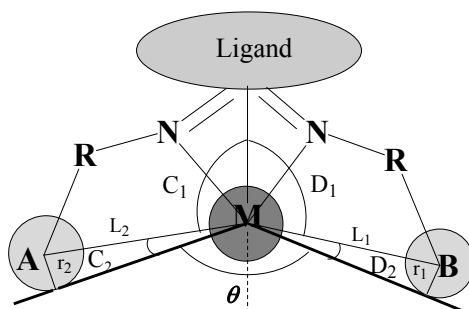


Figure S10. Definition of open cone angle (θ) of complex.

Table S2. The calculated values of effective net charge (Q_{eff}) and open cone angle (θ) for four complexes, respectively.

	D-Me	D-NO₂	B-tBu	E-tBu
$Q(\text{Fe})/e$	0.801	0.797	0.656	0.798
$Q(\text{Cl}_1)/e$	-0.398	-0.401	-0.598	-0.396
$Q(\text{Cl}_2)/e$	-0.403	-0.396	-0.608	-0.402
Effective net charge (Q_{eff}/e)	0.796	0.802	0.646	0.792
Open cone angle (θ) ^o	100.56	82.99	129.25	90.69

References:

- NL. Allinger, U. Burkert, *Molecular Mechanics*, (1982) An American Chemical Society Publication. Washington, DC.
- a) W. Yang, Z. Ma, J. Yi, S. Ahmed, and W.-H. Sun, *J. Comput. Chem.* 40 (2019) 1374–1386; b) W. Yang, S. Ahmed, T. T Fediles, W.-H. Sun, *Catal. Commun.* 132, (2019) 105820–105824; c) W. Yang, T. T Fediles, W.-H. Sun, *J. Comput. Chem.* 41 (2020) 1064–1067.
- S. L. Mayo, B. D. Olafson, W. A. Goddard, *J. Phys. Chem.* 94 (1990) 8897–8909.
- a) S. Ahmed, W. Yang, Z. Ma, W.-H. Sun, *J. Phys. Chem. A* 122 (2018) 9637–9644; b) A. A. Malik, W. Yang, Z. Ma, W.-H. Sun, *Catalysts* 9 (2019) 520–527.
- Yang, W.; Chen, Y.; Sun, W.-H. *Macromol. Chem. Phys.* 215 (2014) 1810–1817.
- J. Yi, W. Yang, W.-H. Sun, *Macromol. Chem. Phys.* 217 (2016) 757–764.